Frequency spectrum of the flicker phenomenon in erythrocytes

F. Brochard, J.F. Lennon

Tome 36 No 11 Novembre 1975

LE JOURNAL DE PHYSIQUE

Classification
Physics Abstracts
9.720

FREQUENCY SPECTRUM OF THE FLICKER PHENOMENON IN ERYTHROCYTES

F. BROCHARD and J. F. LENNON (*)

Laboratoire de Physique des Solides, Université Paris-Sud, Centre d'Orsay, 91405 Orsay, France

(*Reçu le 22 avril 1975, accepté le 20 juin 1975*)

Résumé. — Les globules rouges placés dans des conditions physiologiques normales présentent un phénomène remarquable de scintillement. On a étudié expérimentalement les fonctions de corrélation $G(R_{12}, \omega)$ pour les intensités de scintillement mesurées en deux points r_1 r_2 de la surface de la cellule, à diverses fréquences de filtrage ω. On trouve que la forme de G est universelle et que la portée des corrélations ne fait intervenir qu'une longueur caractéristique $\lambda(\omega)$ variant comme ω^{-n}, où $0{,}12 < n < 0{,}19$. Les mesures de $G(0, \omega)$ (c'est-à-dire en un seul point) montrent une dépendance en ω^{-m}, avec $1{,}3 < m < 1{,}45$. Ces résultats sont ensuite interprétés théoriquement en terme de fluctuations thermiques de l'épaisseur de la cellule. Dans des conditions physiologiques, la tension de surface de la membrane est nulle et la résistance à la déformation est due seulement à une énergie de courbure. On montre que :

a) les fluctuations ont une grande amplitude (une fraction de micron), ce qui est effectivement observé ;

b) la forme détaillée des corrélations est en très bon accord avec la théorie ;

c) la longueur de cohérence $\lambda(\omega)$ doit varier comme $\omega^{-1/6}$;

d) le spectre en un point $G(0, \omega)$ doit varier comme $\omega^{-4/3}$.

Dans notre interprétation on a négligé les effets non linéaires dus à la tension de surface et à l'élasticité de type caoutchouc proposé par Evans. On montre que l'inclusion de ces termes non linéaires nous conduit à un problème semblable au point critique d'un système magnétique (spécial) à deux dimensions. Notre approximation (équivalente à une théorie de champ moyen) ignore essentiellement la correction de l'exposant η introduit par Fisher pour les transitions de phase. Les résultats expérimentaux sont en faveur d'un exposant η très petit.

On conclut qu'une interprétation purement physique du phénomène de scintillement est suffisante, mais que des conditions physiologiques très strictes sont nécessaires pour maintenir la tension de surface nulle.

Abstract. — Red blood cells show a remarkable flicker phenomenon under physiological conditions. We have studied experimentally the correlations functions $G(R_{12}, \omega)$ for the flicker intensities measured at two different points r_1 r_2 on the cell surface, at various filtering frequencies ω. We find that the shape of G is universal and involves only one characteristic length $\lambda(\omega)$ varying like ω^{-n}, where $0.12 < n < 0.19$. Measurements of $G(0, \omega)$ (i.e. at a single point) show an ω^{-m} dependence, where $1.30 < m < 1.45$. These results are then interpreted theoretically in term of thermal fluctuations of the cell thickness. In physiological conditions the membrane surface tension vanishes exactly and the resistance to deformation is mainly due to curvature energy. In this approximation :

a) the fluctuations are of very large amplitude (a fraction of a micron) as required by the observations ;

b) the detailed shape of the correlations is in rather good agreement with the theory ;

c) the scaling length $\lambda(\omega)$ is expected to vary like $\omega^{-1/6}$;

d) the single point spectrum $G(0, \omega)$ should go like $\omega^{-4/3}$.

The approximation involves the neglect of some non linear effects related to surface tension and to the Evans elastic energy. We show that the inclusion of non linear terms leads to a problem related to the critical point of a (special) two dimensional magnetic system. Our approximation (equivalent to a mean field theory) essentially ignores the exponent correction η introduced by Fisher for phase transitions. Thus, the experimental evidence favours a rather small η.

We conclude that a purely physical interpretation of the flicker effect is sufficient, but that rather stringent physiological conditions are required to maintain the zero surface tension which is crucial to the effect.

(*) Institut Pasteur, rue du Dr Roux, Paris 15e.

1. **Introduction.** — As early as 1890 the rhythmic movements of red blood cells (RBC) suspended in solution were observed [1] using ordinary light microscopy. They are best seen with a phase contrast microscope and appear as a shimmering at the junction of the rim and the center of the cells. The impression given is definitely one of turbulence in the cytoplasm [3] and oscillations of the cell membranes. From all of the data available the Flicker Phenomenon appears to be closely correlated with the cell deformability. Under the influence of environmental changes [4, 6, 7] (PH, hypotonic or hypertonic sols, metabolic poisons, temperature, compression...) the red cell loses its discoidal shape. The deformability of the cell membrane is then strongly reduced and the extent of flickering diminishes drastically (Fig. 1).

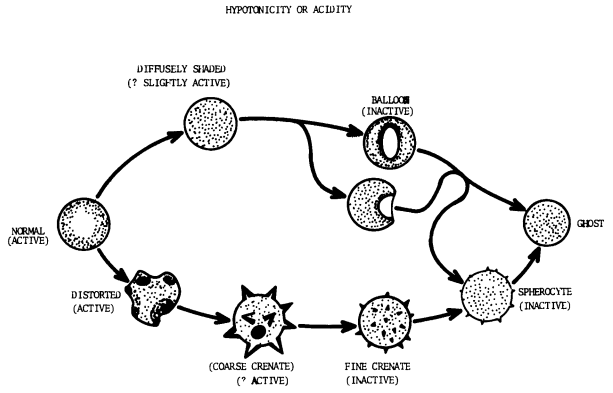

FIG. 1. — Changes in shape of a human erythrocyte and flicker activity after (Blowers *et al.*) [4].

There have been many attempts to explain the vibratory movements of RBC [1, 2, 3, 4, 5] and these fall into two classes :

i) Motion is a fundamental property of the living matter. In general, the cell motions result from the transformation of chemical energy into mechanical energy and are related to the metabolic activity of the cell. Most of the attempts to explain the flicker phenomenon employ this concept. For example :

— Forkner, Zia and Teng [2] claim that the RBC scintillation is the result of molecular movements associated with the oxidation and reduction of large molecules of hemoglobin. Indeed, Flicker has been observed only in intact cells and not in ghosts.

— However Pulvertaft [3] has shown more recently that the cell motion cannot be related to hemoglobin activity since when saturated with carbon monoxide the cell still flickers. In the Pulvertaft picture, the hemoglobin acts only as an indicator, making motion visible. He suggests that the glycolytic metabolism only energizes red cell Flicker. Blowers [4] has shown that Flicker is indeed affected by the same agents that affect active transports and concluded that Flicker is related to glycolisis. However, these results are not quite convincing : the agents used act not only on the active transport, but also on the mechanical properties of the membrane (for instance, some of them transform the discocyte into the echinocyte form, resulting in a spontaneous curvature change).

ii) In the second hypothesis it is proposed that the vibratory motion is not related to an active biological process in the cell, but is only a result of thermal agitation. Parpart and Hoffman [5] suggest that the flicker is a result of Brownian motion or *bombardment of the thin cell membrane by molecules from inside and outside.* The flicker is reduced or disappears if the number of degrees of freedom are reduced (for example if the cells are fixed on a wall, form a rouleau...) or if the viscosity of the plasma is increased.

All these suppositions are based on purely qualitative observations. In order to understand the effect more deeply a quantitative experimental study is necessary. A first attempt in this direction was due to Burton *et al.* [20] : they succeeded in measuring the frequency spectrum of the flicker effect. Unfortunately their accuracy was not sufficient to yield any quantitative conclusions. In the present work, using phase contrast microphotometry, we have measured the frequency spectrum for the intensity of the flicker and the correlations functions $G(R_{12}, \omega)$ for the flicker intensities measured at two different points r_1 r_2 on the cell surface, for a varying filtering frequency ω. We find that a quantitative interpretation of these results can be constructed using the second concept, i.e. that the flicker is a purely physical effect due to thermal fluctuations of the cell thickness.

In section 2, we present a summary of the experimental results. The details of the experimental set up, together with a quantitative study of the influence of environmental changes on flicker, shall be given elsewhere [22].

In section 3, we attempt to interpret quantitatively these experimental results in term of the thermal fluctuations of the cell surface :

In a first part, we study the thermodynamic equilibrium properties of the cell membrane deformations. Helfrich [8] has established that the forces responsible for the biconcave discoidal shape of the RBC are extremely weak. Under these conditions, we show that the spontaneous membranes distortions strongly modulate the cell thickness. In our model, this random thickness modulation is responsible of the scintillations.

We also show that spontaneous deformations are much weaker in the case of a spherical RBC and consequently the flicker should vanish, which is confirmed by experimental observations.

In a second part, we study the dynamical properties of the surface oscillations. We calculate the dispersion relation of the eigenmodes and the dynamical spatial correlation functions $\langle \delta d(r_1)\, \delta d(r_2) \rangle_\omega$, for

the thickness fluctuations measured at two points r_1 r_2 of the cell surface at a frequency ω.

In section 4, we compare these theoretical results with our experimental data.

2. **Experimental study of flicker.** — The flicker effect has been studied many times [1, 2, 3, 4, 5] [20] since its discovery in 1890, but in most cases flicker is only observed and seemed difficult to define. For these reasons, erythrocytes have just been classified into *active cells* or *inactive cells*, the latter showing only very slight shimmering or none at all (Fig. 1). The few attempts [3, 4] in the past to make numerical measurements of the flicker have not been successful. The only result in this direction is due to Burton *et al.* [20], who obtained the first frequency spectrum the flicker by using a continuous motion film recording technique. They concluded that *flicker under normal conditions does not display any significant isolated frequency, but rather is made of a mixture of a large number of low frequencies varying from about* 40 Hz *to zero.* However, their experiments are not sufficiently accurate to lead to quantitative results.

We present here a quantitative study of the flicker phenomenon, based on photometry (inelastic light scattering is less adapted to study the vibratory movements of the RBC because the coherence area is too small ($S \sim 8 \times 8\ \mu^2$)). Microphotometry is also more convenient because we can control the RBC shape.

Among the microphotometry techniques [21], microspectrophotometry by absorption would seem to be, at first sight, the most convenient because of the high absorption of the hemoglobin near 0.415 μ (soret band). However this approach must be avoided because of photochemical effects [22]. Therefore, we chose to use *phase contrast microscopy*. By this technique, we have measured :

— the mean quadratic amplitude of the cell thickness fluctuations $\langle\ |\ \delta d\ |^2\ \rangle$

— the frequency spectrum $\langle\ \delta d^2(\omega)\ \rangle$

— the spatial correlation functions

$$\langle\ \delta d(r_1)\ \delta d(r_2)\ \rangle_\omega$$

for the thickness fluctuations δd measured at two differents points r_1 r_2 of the RBC surface.

2.1 Principle. — The intensity $I(x', y')$ in the image plane of a phase object $\varphi(x, y)$ is given by the relation [23]

$$I(\mathbf{r}', t) = I_0\left[1 + 2\,\frac{\varphi(\mathbf{r}, t)}{a_0}\sin\alpha_0\right]. \qquad (2.1)$$

— α_0 and a_0^2 are the retardation angle and the transmission of the objective phase plate respectively. (In our case, $\alpha = \pi/2$ and $a^2 = 0.25$ for $\lambda = 0.55$ μ.)

— I_0 is the intensity without any dephasing object.

Here, φ is the phase change between a RBC at equilibrium and the deformed RBC ([1]), i.e. :

$$\varphi(\mathbf{r}, t) = \frac{\delta d(\mathbf{r}, t)\ \Delta n(\lambda)}{\lambda} \qquad (2.2)$$

where Δn is the difference between the refractive index of the exterior and interior medium (typically $\Delta n = 7 \times 10^{-2}$ for $\lambda = 0.55$ μ) and $\delta d = d(r, t) - d_0(r)$ is the thickness variation of the RBC.

By using (2.1) and (2.2), we get

$$\delta d(r, t) = 2\,\frac{\delta I}{I_0}(r', t)\,. \qquad (2.3)$$

This formula allows us to determine directly the thickness variation at point **r**, which is the primary result. Then, it is easy to obtain the mean quadratic value of the thickness fluctuations $\langle\ \delta d^2\ \rangle$, the frequency spectrum $\langle\ \delta d^2(\omega)\ \rangle$, and the correlations

$$\langle\ \delta d(r_1)\ \delta d(r_2)\ \rangle_\omega$$

at various filtering frequencies ω. The limit of resolution for r is determined by the microscope (0.3 μ).

2.2 Results. — We have studied the flicker effect in erythrocytes of human, frog and chicken. We give here a summary of the experimental study ; a complete description of the methods and materials used is reported in a separate experimental article [22].

2.2.1 *Determination of the frequency spectrum* $\langle\ \delta d^2(\omega)\ \rangle$. — The light intensity fluctuations $\delta I(\mathbf{r}', t)$ are recorded on a magnetic tape and analyzed by the spectrum analyser which consists of a variable center frequency narrow band filter and a square law detector. The spectral power $\langle\ \delta d^2(\omega)\ \rangle$ is thus plotted as a function of ω, for a frequency range

$$0.2\ \text{Hz} < \omega < 30\ \text{Hz}\,,$$

with a resolution of 0.2 Hz : a typical recording is shown on figure 2 for the case of a human erythrocyte in a log log scale. The law is linear for $\frac{\omega}{2\pi} > 1$ Hz and the slope is $1.30 < m < 1.45$:

$$\delta d^2(\omega) = G(0, \omega) \sim \omega^{-m} \quad 1.3 < m < 1.45\,. \qquad (2.4)$$

For the frog and chicken erythrocytes, the plot of δd^2 versus ω follows the same power law with the same exponent.

2.2.2 *Determination of the mean quadratic fluctuation* $\langle\ \delta d^2\ \rangle$. — The mean quadratic value can be obtained :

— either by the integration of $\langle\ \delta d^2(\omega)\ \rangle$

$$\delta d^2 = \int \delta d^2(\omega)\ \mathrm{d}\omega$$

([1]) We suppose here that φ is entirely due to a thickness variation and not to a fluctuation of refractive index n of the cell interior. This has been verified in the case of the frog RBC ; the depth of field of the microscope is less than the cell thickness d_0 and we find that the light intensity I is time independent within the cell.

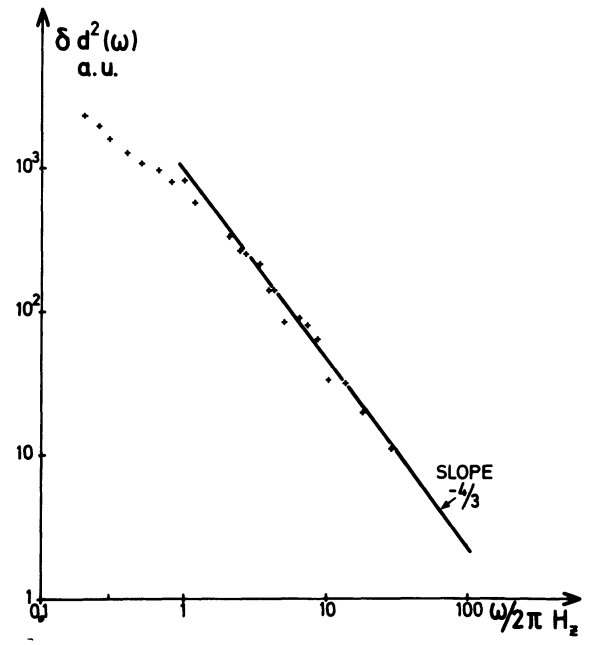

FIG. 2. — A typical frequency spectrum of the thickness fluctuations of a human erythrocyte. We find identical spectra for frog and chicken cells; the only difference is the frequency value below which linearity does not hold.

— or by using a frequency filter with a large band width (0.2-30 Hz).

By these two means, we measured :

$$\sqrt{|\,\delta d\,|^2} = 8 \times 10^{-2}\,\mu \qquad (2.5)$$

for both human and frog RBC. For the chicken RBC, the result is half as large.

2.2.3 *Correlation functions*

$$G(\omega, R_{12}) = \langle\, \delta d(r_1)\, \delta d(r_2)\, \rangle_\omega\,.$$

To measure $G(\omega, R_{12})$, we have to study the flicker simultaneously in two points r_1, r_2. This can be achieved by splitting the image in two with a partially reflective mirror. We filter a frequency ω and we record $\langle\, \delta d_\omega(\mathbf{r}_1)\, \delta d_\omega(\mathbf{r}_2)\, \rangle$ versus $R_{12} = |\,\mathbf{r}_1 - \mathbf{r}_2\,|$. We have studied the correlations at $\frac{\omega}{2\pi} = 4.5$ Hz, 20 Hz and 90 Hz for human, frog and chicken RBC. A typical recording is shown on figure 3*a*.

These correlations functions present two characteristic properties :

i) *The spectrum is universal.* — We find that the shape of the correlation functions is always the same and looks like the function shown figure 3*a* : it is independent of the nature of the RBC, the cell thickness and the frequency for erythrocytes *under normal physiological conditions.* We do not find this typical shape if the RBC is altered (Fig. 3*c*).

It has to be notice that for frog and chicken, the shape is not modified in the region of the nucleus (Fig. 3*b*).

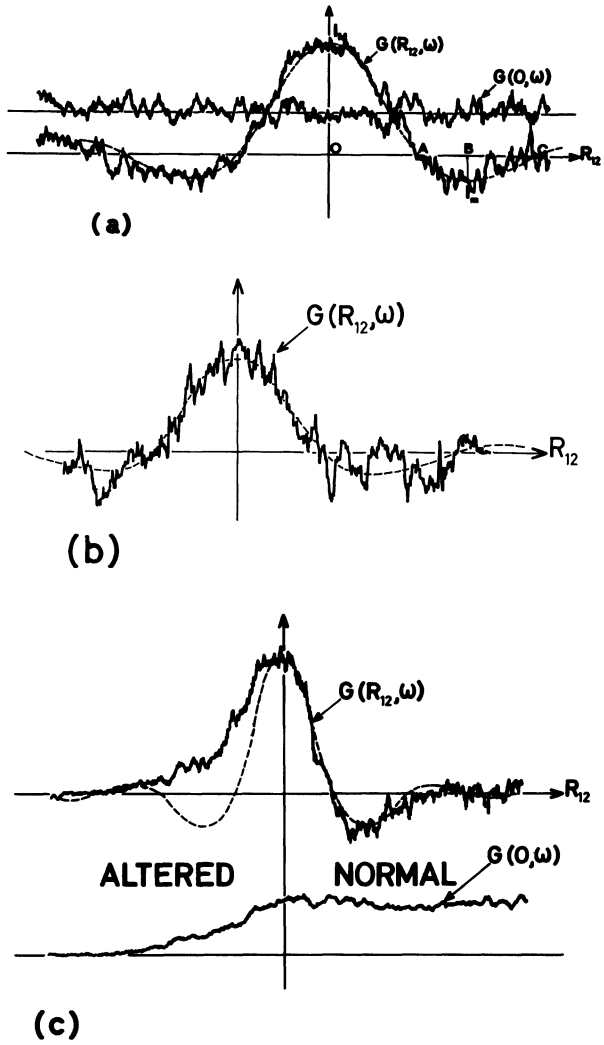

FIG. 3. — Typical recordings versus $R_{12} = r_1 - r_2$ of the correlation function $G(R_{12}, \omega)$ for the flicker intensities measured at two different points r_1 (fixe) r_2 (variable) on the cell surface at various ω ($\omega/2\pi$ = 4.5, 20, 90 Hz) for frog chicken and human erythrocytes. The dotted line is the theoretical curve (Fig. 8). The other curve $G(0, \omega)$ is the flicker intensity at the single point r_1 and verifies that Flicker is not modified during the experiment; *a* : erythrocyte in normal conditions, *b* : correlations in the nucleus region (for a frog RBC); *c* : altered erythrocyte : as the cell is osmotically swollen, the flicker intensity $G(0, \omega)$ goes to zero and the shape of $G(R_{12}, \omega)$ is different (no oscillations).

ii) *The correlations involve only one relevant length* $\lambda(\omega)$. — All the correlation function curves can be superposed by a scaling change which involves one caracteristic length $\lambda(\omega)$. By varying ω and studing the correlations around *the same point* r_1, we have ploted $\lambda(\omega)$ versus ω (Fig. 4) for human and chicken. We find a linear dependence in log log scale, with a slope $0.12 < n < 0.19$:

$$\lambda(\omega) \sim \omega^{-n} \quad 0.12 < n < 0.19\,. \qquad (2.6)$$

3. **Interprétation.** — 3.1 SPONTANEOUS RBC DEFORMATIONS AND RELATED ENERGIES. — 3.1.1 *Description of red blood cells* (RBC). — RBC [7] are usually described as bags filled with hemoglobin

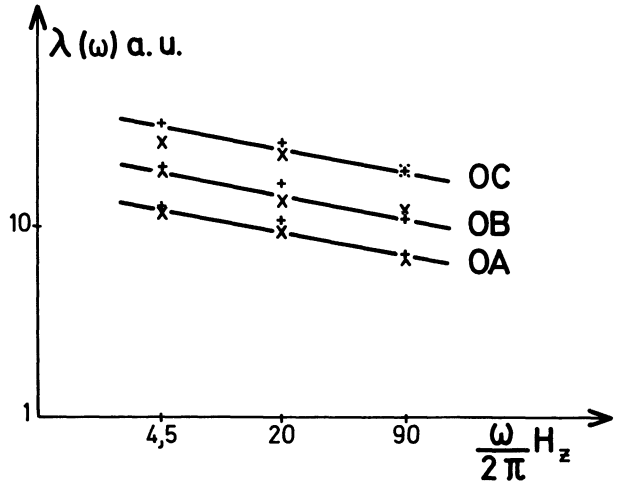

FIG. 4. — Frequency dependence of the correlation range $\lambda(\omega)$.

solution. The mature mammalian erythrocyte has no nucleus (Fig. 5), but the bird and avian erythrocytes have a nucleus. The cell membrane is complex and contains numerous proteins embedded in a lipid bilayer.

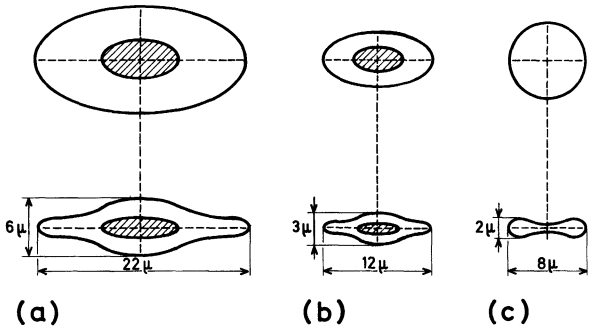

FIG. 5. — Schematic representation of frog (*a*), chicken (*b*) and human (*c*) erythrocytes.

The study of the RBC rheology [10, 16] show that these cells are deformable :

— the membrane is a two dimensional liquid [9, 10] (no resistance to shear),

— the cell interior is, to a first approximation, a newtonian fluid [16] of viscosity $\eta \simeq 6$ cP.

3.1.2 *Elastic properties of the membrane.* — Human RBC possess a biconcave-discoid shape (8 μ × 2 μ) under normal physiological conditions (Fig. 5*c*). Various attempts [8, 11, 12] have been made to explain this form. It seems now established that the elasticity of the bounding membrane and the enclosed volume control the shape. Recently, an elastic theory of lipid bilayers was proposed by Helfrich [8] and used with success to describe the transition between the biconcave disk and the sphere via osmotic changes of the enclosed volume.

If the enclosed volume V_i is reduced below the critical volume V_c, characterized by a vanishing total tension in the spherical bilayer,. *the cell shape is controlled entirely by curvature elasticity.* This conclusion of Canham [10] re-established by Helfrich (2) [3] is supported by the observation that the membrane area remains practically constant in the transition disk sphere.

We apply now the same conceptions to discuss the RBC spontaneous deformations around its discoidal equilibrium shape. To simplify, we substitute for the disk two membranes of surface S (8 μ × 8 μ) separated by a distance d (2 μ) as shown in figure 6, and we neglect boundary effects.

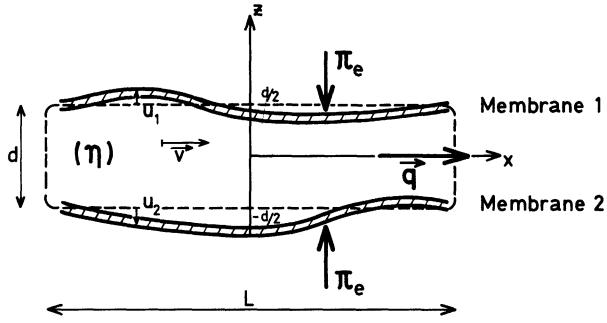

FIG. 6. — Theoretical model for study of the thickness fluctuations of a human erythrocyte.

Let us now evaluate the free energy associated to the RBC deformation. For a thickness $d \simeq 2$ μ, the interactions (Van der Waals, electrostatic) between bilayers are negligible and the fluctuations of membrane [1] and [2] are decoupled. The free energy is the sum of the elastic energy of the two membranes

$$F = F_1 + F_2 .$$

i) One essential contribution to F_1 and F_2 is the *curvature* energy. In terms of u_1, the displacement of membrane 1, the elastic energy may be written as :

$$F_1 = \int_{S_1} \frac{1}{2} K \left[\frac{\partial^2 u_1}{\partial x^2} + \frac{\partial^2 u_1}{\partial y^2} \right]^2 \mathrm{d}S . \qquad (3.1)$$

As estimation of the elastic modulus K, we can take $K = K_1 \times e$, where K_1 [14] is the Frank curvature modulus for a liquid crystal and e the bilayer thickness. As $K_1 \sim \frac{k_B T_c}{a}$, where $k_B T_c$ is a typical molecular interaction and a is an intermolecular length,

$$K \simeq k_B T_c \times \frac{e}{a} (\simeq 5 \times 10^{-13} \text{ ergs}) . \qquad (3.2)$$

ii) It is essential to realize that surface tension term does not contribute to the free energy in order u^2.

(2) In the Canham description, one finds in fact both an oblate and a prolate shape. Of the two shapes, the elongated one has the lower energy. Helfrich and Deuling [13] have shown that the membrane must have a spontaneous curvature opposite to the curvature of the sphere if flattened forms rather than elongated ones are to be stable.

Effectively, the membrane energy $E(\Sigma)$ as a function of the total area (Σ) is extremal for $\Sigma = \Sigma_0$, the equilibrium value. Then, for Σ close to Σ_0, we may write :

$$E(\Sigma) = \frac{1}{2} C(\Sigma - \Sigma_0)^2 + E_0 \qquad (3.3)$$

In our case,

$$\Sigma - \Sigma_0 \sim \int dS \frac{1}{2}\left[\left(\frac{\partial u_1}{\partial x}\right)^2 + \left(\frac{\partial u_1}{\partial y}\right)^2 + \left(\frac{\partial u_2}{\partial x}\right)^2 + \left(\frac{\partial u_2}{\partial y}\right)^2\right].$$

Thus $\Sigma - \Sigma_0$ is of the 2nd order in u_1 and u_2 and the term $E - E_0$ is of the fourth order in $u_1 . u_2$.

A similar non linear effect is associated with the two dimensional rubber elasticity proposed by Evans [24]; the membrane possesses a proteic rigid component giving a finite resistance to stretch at constant area. The Evans energy density is of the form

$$F_E = \frac{\mu}{4}(l^2 + l^{-2} - 2)$$

where μ is an elastic coefficient, and l is the longitudinal extension. For a wave like deformation $u(x)$ of the membrane, we have :

$$l = \sqrt{1 + \left(\frac{du}{dx}\right)^2} \cong 1 + \frac{1}{2}\left(\frac{du}{dx}\right)^2 .$$

The resulting energy (for l close to 1) is

$$F_E = \mu(l - 1)^2 \cong \frac{\mu}{4}\left(\frac{du}{dx}\right)^4 . \qquad (3.4)$$

This is again of fourth order in the amplitude.

The problem of fluctuations in a sheet described by this type of free energy is very special : *in the harmonic approximation, the curvature terms are the only ones present.* But, as soon as the tilt angles $\left(\frac{\partial u}{\partial x}\right)$ become finite, the non linear surface energy terms become important ([3]).

In the next paragraph, we present a simple discussion based on the harmonic terms alone. This turns out to be in rather good agreement with experiment. In section 4, we come back to the problem of anharmonic corrections.

3.2 STATICS OF THERMAL FLUCTUATIONS IN THE HARMONIC APPROXIMATION. — The calculation of the amplitude of membrane fluctuations has been described by Papoular and de Gennes [15] for the general case. We derive it here for our simpler case, when only the curvature energy is relevant.

It is convenient to analyze u_1 and u_2 in Fourier components, defined by

$$u_q = \int u(r)\, e^{iqr}\, d_2\mathbf{r} .$$

In term of these Fourier components, F becomes

$$F = \frac{1}{2S}\sum_q Kq^4[u_1^2(q) + u_2^2(q)] . \qquad (3.5)$$

We can now derive the thermal average of $u_1^2(q)$ and $u_2^2(q)$ simply from the equipartition theorem

$$\langle\, |u_1^2(q)|\, \rangle = \langle\, |u_2(q)|^2\, \rangle = S\frac{k_B T}{Kq^4} .$$

This yields, for the fluctuations of the thickness $\delta d = u_1 - u_2$,

$$\langle\, |\delta d(q)|^2\, \rangle = 2\langle u_1^2(q)\rangle = 2S\frac{k_B T}{Kq^4} . \qquad (3.6)$$

By integration of $\langle \delta d^2(q) \rangle$ over the wave vectors q, one obtains the thermal average of the thickness fluctuations :

$$\langle\, |\delta d|^2\, \rangle = \frac{1}{(2\pi)^2 S}\int_{\pi/L}^{\infty} d_2 q \langle\, |\delta d(q)|^2\, \rangle .$$

This integral is strongly divergent at small q but the cell diameter L gives a lower cut off π/L.

Using for K the estimation (3.2), one gets :

$$\delta d \sim \frac{L}{\pi^{3/2}}\sqrt{\frac{a}{e}} \sim 0.3\ \mu . \qquad (3.7)$$

Remark 1 : these thickness fluctuations are comparable to the RBC dimensions and easily detectable : the eye is sensitive to light intensity fluctuations $\frac{\delta I}{I} \sim \frac{1}{100}$; if ε is the absorption coefficient of hemoglobin, $\frac{\delta I}{I} \simeq \varepsilon\, \delta d$, i.e. $\frac{\delta I}{I} \simeq 5\,\%$ with $\varepsilon = 1\,500$ and $\delta d = 0.3\ \mu$. However, these estimates will be reduced by the non linear terms (see section 4).

Remark 2 : if the red cell is swollen via osmotic change of the enclosed volume V and becomes spherical, the surface Σ and the volume V are coupled. The energy $E(\Sigma)$ is no longer stationary with respect to Σ and V separately. We must now include in (3.1) a surface tension term :

$$F_1 = \int_{S_1} \frac{1}{2}\sigma\left[\left(\frac{\partial u_1}{\partial x}\right)^2 + \left(\frac{\partial u_1}{\partial y}\right)^2\right] dS \qquad (3.8)$$

where the surface tension $\sigma \simeq \frac{k_B T_c}{a^2}$ ($\simeq 10^2$ dynes/cm) ;

([3]) We are indebted to two referees for pointing out to us the relative magnitude of the non linear terms.

$k_B T_c$ is a typical molecular interaction energy and a is an intermolecular length.

Taking into account this additional term, the thermal average $\langle | \delta d(q) |^2 \rangle$ is now given by

$$\langle | \delta d(q) |^2 \rangle = 2 S \frac{k_B T}{(Kq^4 + \sigma q^2)}. \quad (3.9)$$

The divergence at small q is reduced. By integration, we get the mean quadratic thickness fluctuations :

$$\langle | \delta d |^2 \rangle = \frac{2 k_B T}{(2\pi)^2} \int_{\pi/L}^{\pi/a} \frac{2\pi q \, dq}{\sigma q^2 + K q^4}.$$

The divergence is only logarithmic ; the upper cut off is given by a molecular length a and the integration leads to :

$$\langle | \delta d |^2 \rangle = \frac{k_B T}{\pi\sigma} \operatorname{Log} \frac{L}{a}. \quad (3.10)$$

With $\sigma \sim \frac{kT}{a^2}$, one gets $\delta d \sim a$, a *molecular length* ($\simeq$ 10 Å). Thus, as soon as surface tension appears, the amplitude of the oscillations diminishes greatly. It becomes comparable to the amplitude of ripples on a fluid interface (soap bubble) and the flicker effect disappears, which is what is observed.

3.3 DYNAMICS OF THE RBC DEFORMATIONS IN THE HARMONIC APPROXIMATION. — The oscillation of the membrane induces flow inside and outside the cell. Therefore to study the dynamical behaviour of the cell deformations we have to describe both :

— the viscoelastic properties of the membrane,

— the equations governing the flow of the cytoplasm and the cell environment.

From these equation of motion we calculate the power spectrum $\langle | \delta d(q, \omega) |^2 \rangle$ of the thickness fluctuations, using as a theoretical framework linear response theory and the fluctuation-dissipation theorem. We also derive the spatial correlation function $\langle \delta d(r_1) \, \delta d(r_2) \rangle_\omega$, which can be determined from phase contrast spectrophotometric measurements.

3.3.1 RBC *Motion equations.* — i) *Viscoelastic properties of the membrane.* — The viscoelastic restoring forces acting upon the membrane deformations are given by the functional derivative of the free energy F (3.1)

$$f_i = - \frac{\delta F}{\delta u_i} = K \left[\frac{\partial^4 u_i}{\partial x^4} + \frac{\partial^4 u_i}{\partial y^4} \right]. \quad (3.11)$$

The frictional forces are given by the dissipation function TS, which measures the energy dissipated as the cell is deformed. By analogy with nematic liquid crystals, we may write

$$T\dot{S} = \int \gamma \left[\left(\frac{\partial \dot{u}}{\partial x} \right)^2 + \left(\frac{\partial \dot{u}}{\partial y} \right)^2 \right] dS. \quad (3.12)$$

As an estimation of γ, we take $\gamma = \gamma_1 \times e$.

γ_1 is the Leslie viscosity [14] coefficient of nematics, associated with molecular rotation.

e is the membrane thickness ($e \simeq 50$ Å).

With $\gamma_1 = 0.1$ P, $e = 50$ Å, one obtains

$$\gamma \simeq 10^{-6} \text{ cP}.$$

The dissipation in the membrane is therefore negligible (except for ripples of wave length comparable to e, which are not discussed here).

ii) *Induced flow.* — a) *In the cell.* — The interior of the cell is a Newtonian fluid [16] in a first approximation ; its motion is governed by the Navier Stockes equations. In the limit of small amplitude motions discussed here, these equations can be linearized. If p is the pressure of the enclosed fluid and v the velocity, they can be written as

$$\operatorname{div} \mathbf{v} = 0 \quad (3.13)$$

$$\rho \frac{\partial \mathbf{v}}{\partial t} = \eta \, \Delta \mathbf{v} - \mathbf{grad}\, p. \quad (3.14)$$

A typical value for η is $\eta = 6$ cP [16].

b) *In the cell environment.* — The viscosity of the environment is smaller than the cytoplasm viscosity ($\sim \eta/6$). Moreover, the velocity gradient outside the cell is smaller because the flow extends over a volume L^3 instead of $L^2 d$, L being the cell diameter and d the thickness. This flow leads to frictional dissipation outside the cell approximatively twenty times smaller than the dissipation within the cell and we shall neglect it in the following ($\eta_e \simeq 0$), i.e. an isolated cell.

iii) RBC *Motion equations.* — As a model, the red blood cell may be described as a liquid film of dimensions (L, d), bounded on both surfaces by a lipid bilayer. The geometric parameters are represented on figure 6.

The dynamics are entirely defined by eq. (3.13), (3.14) and the boundary conditions at the cell surface requiring :

a) The equilibrium between the viscous stress σ_{zz_i} exerted by the fluid on the membrane and the restoring elastic force f_i defined by (3.11), written as :

$$\sigma_{zz_1} = 2\eta \frac{\partial v_z}{\partial z}\bigg|_{d/2} + p\left(\frac{d}{2}\right) = K\left(\frac{\partial^4 u_1}{\partial x^4} + \frac{\partial^4 u_1}{\partial y^4}\right)$$

$$\sigma_{zz_2} = 2\eta \frac{\partial v_z}{\partial z}\bigg|_{-d/2} - p\left(-\frac{d}{2}\right) = K\left(\frac{\partial^4 u_2}{\partial x^4} + \frac{\partial^4 u_2}{\partial y^4}\right). \quad (3.15)$$

b) The continuity of the velocities of the fluid and the membrane :

$$v_z\left(\frac{d}{2}\right) = \frac{\partial u_1}{\partial t}; \quad v_z\left(-\frac{d}{2}\right) = \frac{\partial u_2}{\partial t}$$

$$v_\perp\left(\pm\frac{d}{2}\right) = 0 \quad (3.16)$$

(membrane stretching modulus is ∞ : S = const.).

3.3.2 *Eigenmodes of deformations : frequencies and power spectrum* $\langle |\delta d(q,\omega)|^2 \rangle$. — i) *Principle.* — Suppose that we apply on both membranes an external pressure $\pi_e(r, t)$. This adds to the surface free energy a contribution of $\int d_2\mathbf{r}(u_1 - u_2)\,\pi_e(r, t)$. The elastic restoring force is thus modified according to (3.11) and the boundary condition (3.15) becomes :

$$\begin{aligned} \sigma_{zz_1} &= f_1 - \pi_e \\ \sigma_{zz_2} &= f_2 + \pi_e \,. \end{aligned} \qquad (3.15bis)$$

From the equations of motion, we find that the thickness d is modified ($d \to d + \delta d$) at all points. The most general form of δd is

$$\delta d = u_1(r, t) - u_2(r, t) = \int_S d\mathbf{r}' \int_{-\infty}^{t} \chi(r - r', t - t')\,\pi_e(r', t')\,dt' \,.$$

If we take $\pi_e = \pi\, e^{iqx}\, e^{i\omega t}$, this leads to

$$\delta d(q, \omega) = \chi(q, \omega)\,\pi S \,. \qquad (3.17)$$

From the response function $\chi(q, \omega)$ defined by (3.17), we can derive [17] :

— the eigenfrequencies of the deformation modes which correspond to the poles of χ,

— the power spectrum of the thickness fluctuations $\langle |\delta d(q, \omega)|^2 \rangle$, related to $\chi(q, \omega)$ by the fluctuation dissipation theorem. In the limit of interest here $\hbar\omega \ll k_B T$, this reduces to

$$\langle |\delta d(q, \omega)|^2 \rangle = -\frac{k_B T}{\pi\omega} \operatorname{Im} \chi(q, \omega) \,. \qquad (3.18)$$

Our aim is to solve the motion equations in the presence of an external pressure $\pi_e(r, t)$. We find the resulting δd and thus obtain $\chi(q, \omega)$. Finally, by (3.18), we shall obtain $\langle |\delta d(q, \omega)|^2 \rangle$.

ii) *Eigenmodes and response functions.* — When the external pressure $\pi_e(q, \omega) = \pi\, e^{iqx + i\omega t}$ is applied, the general solutions of eq. (3.13), (3.14) for the velocity and the pressure of the fluid enclosed in the cell are of the form

$$\begin{aligned} v_x &= (iqA\, e^{qz} + iqB\, e^{-qz} - lC\, e^{lz} + lD\, e^{-lz})\, e^{iqx + \alpha t} \\ v_z &= (qA\, e^{qz} - qB\, e^{-qz} + iqC\, e^{lz} + iqD\, e^{-lz})\, e^{iqx + \alpha t} \\ p &= -\alpha\rho(A\, e^{qz} + B\, e^{-qz})\, e^{iqx + \alpha t} \end{aligned} \qquad (3.19)$$

with $l^2 = q^2 + \dfrac{\alpha\rho}{\eta}$ and $\alpha = i\omega$.

Inserting this solution in the boundary eq. (3.15*bis*), (3.16) we can calculate A, B, C, D in term of π and arrive at $\delta d = u_1 - u_2 = \chi(q, \omega)\,\pi$. The general case is complex, but it is sufficient to know the two limits $qd \gg 1$ and $qd < 1$ to investigate the characteristic features of the dynamical behaviour.

a) *Limit* $qd \gg 1$. — This case is identical to the case of an isolated membrane because the penetration depth of a surface wave is on the order of q^{-1}, as shown in the general solution (3.19). The frequency spectrum of the surface fluctuations of an isolated membrane has been calculated for non vanishing surface tension [18]. For that case it is found that the ripples at the surface propagate with frequency ($\omega_{12} = \pm \sigma q^{3/2}$). In our model, because the surface tension is zero and the curvature energy is extremely weak, these propagative modes become purely diffusive modes.

We find for the response function

$$\chi(q, \omega) = \frac{\tau_0 q^2 S_0}{\rho} \frac{\sqrt[+]{1 + 2S_0} - 1}{D(S_0)}$$

$$D(S_0) = S_0^2 \sqrt[+]{1 + 2S_0} + (y + \Gamma S_0)\left(\sqrt[+]{1 + 2S_0} - 1\right)$$

where

$$\tau_0 = \frac{\rho}{2\eta q^2}, \quad S_0 = -i\omega\tau_0, \quad y = \frac{Kq\rho}{4\eta^2}, \quad \Gamma = \frac{\gamma q}{2\eta}$$

($\sqrt[+]{\ }$ designates the root with a positive real part).

α) *Fluctuation modes.* — For a wave vector q, we find two eigenfrequencies which are the roots of $D(S_0) = 0$.

1. *Root* $S_0 \ll 1$: *Slow mode.* — For $S_0 \ll 1$,

$$D(S_0) = S_0^2 + (1 + \Gamma) S_0 + y = 0 \,.$$

As predicted in section 3.1, the dissipation in the membrane is negligible ($\Gamma \sim eq \ll 1$) and

$$\omega_1 = i\frac{Kq^3}{2\eta} \quad \textit{Slow Mode} \,. \qquad (3.20)$$

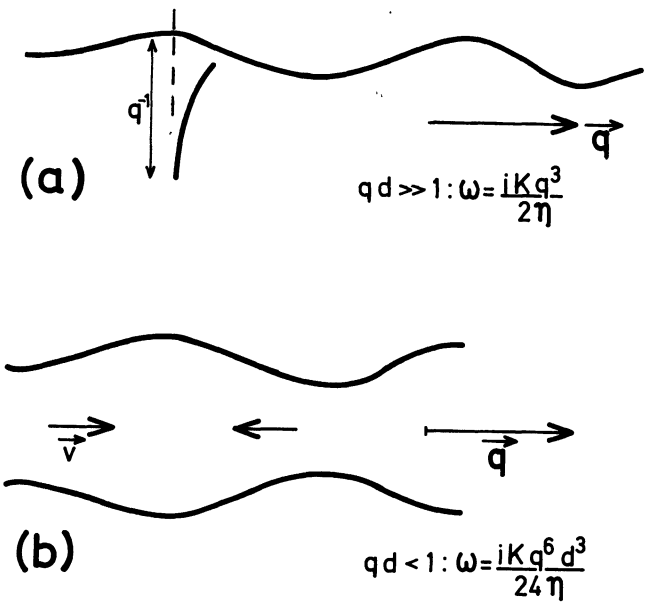

FIG. 7. — Eigenmodes for the thickness fluctuations : *a* : in the limit $qd \gg 1$ (identical to the case of *one* isolated membrane separating two fluids) ; *b* : in the limit $qd < 1$ (similar to the peristaltic modes of a soap film).

Typically $\omega \simeq 15\ s^{-1}$ for $q \simeq \pi/d$ with $d = 2\ \mu$, $K = 5 \times 10^{-13}$ ergs, $\eta = 6$ cP.

In this mode, represented on figure 7, the elastic restoring force is balanced by the frictional force. All inertial effect in the fluid are negligible.

2. *Root* $S_0 \sim 1$: *Fast mode.* — The second eigenfrequency is

$$\omega_2 = i\eta q^2/\rho\ .$$

Typically $\omega \sim 10^7\ s^{-1}$ for $q \simeq \pi/d$.

For this mode, the inertial effects are dominant.

β) *Power spectrum* $P(\omega) = \langle\ |\ \delta d(q, \omega)\ |^2\ \rangle$. — The power spectrum derived from χ by eq. (3.18) is :

$$P(\omega) \simeq 2\,S\frac{k_B\,T}{\pi}\,\frac{1}{2\,\eta q}\,\frac{1}{\omega^2 + \left(\frac{Kq^3}{2\,\eta}\right)^2}\ . \qquad (3.21)$$

The spectrum is thus entirely dominated by the *slow mode.* A check of eq. (3.21) is obtained if we investigate the integrated intensity :

$$\int_{-\infty}^{+\infty} P(\omega)\,d\omega = 2\,S\frac{k_B\,T}{Kq^4}\ .$$

This agrees with the equipartition theorem result (3.6).

b) *Limit* $qd < 1$. — This limit is the most interesting one because the fluctuations are very large for small wave vector ($u_q^2 \sim q^{-4}$).

Here also the spectrum is dominated by the slow mode and we may ignore completely the contribution of the fast mode ($\omega_2 = i\eta q^2/\rho$).

We find for the response function

$$\chi = \frac{Sq^2\,d^3/24\,\eta}{i\omega + \frac{Kq^6\,d^3}{24\,\eta}}\ .$$

α) *Eigenmode.* — The pole of χ gives the eigenfrequency of the deformation mode represented on figure 4*b* :

$$\omega = \frac{iKq^6\,d^3}{24\,\eta}\ . \qquad (3.22)$$

Typically,

$$\text{for } q = \frac{\pi}{d}, \quad \omega = 45\ s^{-1} \quad (d = 2\ \mu)$$

$$\text{for } q = 2\frac{\pi}{L}, \quad \omega = 0.5\ s^{-1} \quad (L = 8\ \mu)\ .$$

This mode is similar to the *peristaltic* mode of a soap film [19].

β) *Power spectrum.* — For the power spectrum, we find by using (3.18)

$$\langle\ |\ \delta d(q, \omega)\ |^2\ \rangle = \frac{SkT}{\pi}\,\frac{q^2\,d^3}{12\,\eta}\,\frac{1}{\omega^2 + \left(\frac{Kq^6\,d^3}{24\,\eta}\right)^2}\ . \qquad (3.23)$$

For the integrated intensity :

$$\langle\ |\ \delta d(q)\ |^2\ \rangle = \int \langle\ |\ \delta d(q, \omega)\ |^2\ \rangle\ d\omega$$

we find the equipartition result (3.6).

Remark : For both limits, the frequencies are purely imaginary : a deformed cell returns to its equilibrium shape without any oscillations.

3.3.3 *Spatial correlations*

$$G(R_{12}, \omega) = \langle\ \delta d(r_1)\ \delta d(r_2)\ \rangle_\omega\ .$$

We derive here the spatial dependence of the correlation function between values of δd_ω measured at two different points r_1 and r_2 for a frequency ω. As discussed in the experimental section a knowledge of the dynamic spatial correlation function seems to be the best way to investigate the dynamical behaviour of the flicker.

$G(R_{12}, \omega)$ is the Fourier transform of $\langle\ |\ \delta d(q, \omega)\ |^2\ \rangle$, i.e. :

$$G(R_{12}, \omega) = \frac{1}{(2\,\pi)^2\,S}\int \langle\ |\ \delta d(q, \omega)\ |^2\ \rangle\ e^{iq(r_1 - r_2)}\ d_2\mathbf{q} \qquad (3.24)$$

where $R_{12} = |\ \mathbf{r}_1 - \mathbf{r}_2\ |$.

At low frequency $\omega < \frac{K}{24\,\eta}\,\frac{\pi^6}{d^3}$ ($\simeq 45\ s^{-1}$), the correlations are almost entirely determined by the modes $qd < 1$ and we can take the result (3.23) for $\langle\ |\ \delta d(q, \omega)\ |^2\ \rangle$. If θ is the angle between $\mathbf{q}$ and $\mathbf{r}_1 - \mathbf{r}_2$, this leads to :

$$G(\omega, R_{12}) = \frac{k_B\,Td^3}{(2\,\pi)^3\,6\,\eta}\int_0^{2\pi} d\theta \int_0^{\infty} \frac{e^{iqR_{12}\cos\theta}\,q^3\,dq}{\omega^2 + \left(\frac{Kd^3}{24\,\eta}\right)^2 q^{12}} \qquad (3.25)$$

It is convenient to define a characteristic length

$$\lambda_\omega = \left(\frac{Kd^3}{24\,\eta\omega}\right)^{1/6}\ . \qquad (3.26)$$

Substituting $q' = \lambda_\omega\,q$ leads us to

$$G(\omega, R_{12}) = \frac{k_B\,Td^3\,\lambda_\omega^4}{(2\,\pi)^3\,6\,\eta\omega^2} \times$$

$$\times \int_0^{2\pi} d\theta \int_0^{\infty} \frac{\exp\left(iq'\frac{R_{12}}{\lambda_\omega}\cos\theta\right)}{1 + q'^{12}}\,q'^3\,dq'\ . \qquad (3.27)$$

The main result can be considered at this point : this expression (3.27) shows that $G(\omega, R_{12})$ is an *homogeneous function,* which can be written as

$$G(\omega, R_{12}) = G(\omega, 0)\ f\left(\frac{R_{12}}{\lambda_\omega}\right) \qquad (3.28)$$

with $f(0) = 1$

and $$G(\omega, 0) \sim \omega^{-4/3}$$

$f(R_{12}/\lambda_\omega)$ is a universal function of the ratio R_{12}/λ_ω, which we have calculated numerically. f is represented on figure 8 : it is an oscillating decreasing function.

Remark : The expression (3.27) for $G(\omega, R_{12})$ is valid only for :

$$\omega > \omega_0 = \frac{K}{24\,\eta}\, d^3 \left(\frac{\pi}{L}\right)^6 \quad (\simeq 10^{-2}\ \mathrm{s}^{-1}) .$$

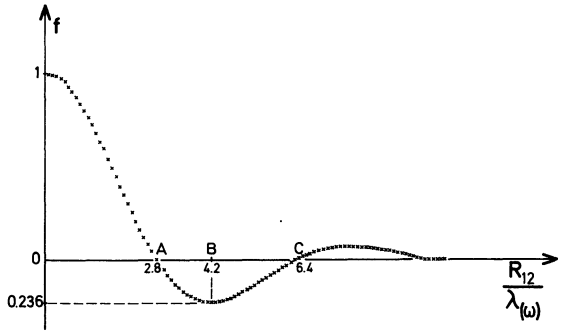

FIG. 8. — Dependence in reduced length $R_{12}/\lambda(\omega)$ of the normalized spatial correlation functions $f = \frac{G(R_{12}, \omega)}{G(0, \omega)}$, where $G(R_{12,\omega}) = \langle\, \delta d(r_1)\, \delta d(r_2)\, \rangle_\omega$ characterizes the correlation for the thickness fluctuations δd at two different points r_1 r_2 on the cell surface at frequency ω and $G(0, \omega)$ measures the fluctuations at a single point r.

At lower frequencies, the cut off $q = \frac{\pi}{L}$ in the q integral has to be taken into account.

Conclusion. — 1° The correlation function

$$G(\omega, R_{12}) = \langle\, \delta d(r_1) \times \delta d(r_2)\, \rangle_\omega$$

is an homogeneous function :

$$G(\omega, R_{12}) \sim \omega^{-4/3}\, f(R_{12}\, \omega^{1/6})$$

where $f(u)$ is an oscillating strongly decreasing function (Fig. 8).

2° The *range of the correlations* involve only one characteristic length λ_ω (3.26). λ_ω is an extremely weak function of ω, which varies as $\omega^{-1/6}$. By taking $K = 5 \times 10^{-13}$, $d = 2\ \mu$, $\eta = 6$ cP, we find :

$$\lambda_\omega = 0.68\ \mu \quad \text{for} \quad \omega = 30\ \mathrm{s}^{-1}$$
$$\lambda_\omega = 0.59\ \mu \quad \text{for} \quad \omega = 60\ \mathrm{s}^{-1} .$$

4. **Discussion of the harmonic approximation.** — 4.1 COMPARISON WITH EXPERIMENT. — The harmonic model explains surprisingly well the main characteristics of the flicker phenomenon.

4.1.1 *The order of magnitude of the cell thickness fluctuations* $\langle\, \delta d^2\, \rangle$. — For both human and frog RBC, we have measured $\delta d^2 = 8 \times 10^{-2}\ \mu$. The order of magnitude of $\langle\, \delta d^2\, \rangle$ is in agreement with the theoretical prediction (3.7). We expect the fluctuations to be larger for the frog RBC ($L = 20\ \mu$) than for the human RBC ($L = 8\ \mu$). However, if the nucleus in the first case acts as a rigid part, δd has to be zero in the center and the lowest wave vector is $2\,\pi/L$ instead of π/L. This argument explains also why the fluctuations for chicken RBC are smaller than for human RBC, in spite of they have same dimensions (Fig. 5).

4.1.2 *Their frequency spectrum versus* ω. — The power law (2.4) $\delta d^2 \sim \omega^{-m}$, $1.3 < m < 1.45$ is in good agreement with the theoretical predictions (3.28) :

$$\delta d^2(\omega) = G(0, \omega) \sim \omega^{-4/3} .$$

On the typical recording of figure 2, $\delta d^2(\omega)$ remains finite as ω tends to zero. The convergence is due to the cut off $q = \pi/L$ in (3.27) and this effect becomes signifiant for :

$$\omega < \frac{K}{24\,\eta} \left(\frac{\pi}{L}\right)^6 d^3 \simeq 10^{-2}\ \mathrm{s}^{-1} .$$

Experimentally, the saturation is observed at very low frequencies.

4.1.3 *The characteristic properties of the spatial correlation functions.* — These correlation functions present two characteristic properties :

a) *The shape of G is universal.* — The shape of the correlation functions is always the same and looks like the theoretical shape function f (Fig. 8); it is independent of the nature of the RBC, the cell thickness and the frequency for erythrocytes *under normal physiological conditions.* We don't find this typical shape if the RBC is altered (Fig. 3*c*).

To fit quantitatively the shape of the correlation function with the theoretical function f plotted on figure 8, we calculate $\frac{OB}{OA}$, $\frac{OC}{OA}$, $\frac{I_M}{I_m}$ (O, A, B, C define the positions of the zeros and extrema of G, I_M and I_m the extremum values as indicated on figure 3*a*. The mean value of these ratios is reported on table I.

TABLE I

	Human	Frog	Chicken	Accuray	Theory
	—	—	—	—	—
$\langle$ OB/OA $\rangle$	1.5	1.6	1.56	± 0.3	1.5
$\langle$ OC/OA $\rangle$	2.54	2.72	2.34	± 0.5	2.28
$\langle\, I_M/I_m\, \rangle$	4.89	4.29	4.05	± 1	4.23

The shape of the correlation function is *universal* and for the twenty curves studied, the *fit* with the *theoretical function f* has been verified.

b) *The correlations involve only one relevant length* $\lambda(\omega)$. — All the correlation function curves can be

superposed by a scaling change which involves one characteristic length $\lambda(\omega)$. The plot of $\lambda(\omega)$ versus ω (Fig. 4) is in good agreement with the theoretical law $\lambda(\omega) \sim \omega^{-1/6}$.

The absolute value of λ leads to a determination of the curvature modulus K. $\lambda(\omega)$ is defined experimentally by :

$$\lambda(\omega) = \frac{OA}{2.8}\left(= \frac{OB}{4.2} = \frac{OC}{6.4}\right).$$

If we compare the measured value to the expected value

$$\lambda_\omega = \left(\frac{Kd^3}{24\,\eta\omega}\right)^{1/6},$$

we can deduce K if we know η and d. For η, we can take $\eta = 6$ cP (3.16). For d, we have unfortunately no independent measure and we have to take an approximative value. We find :

1° For human erythocytes, $\lambda = 0.3\,\mu$ at 20 Hz for the five cells studied. There is no dispersion in the λ value because the correlations are always studied in the center of the cell (i.e. same thickness d). This leads to

$$Kd^3 = 9.8 \times 10^{-13}\ \text{ergs} \times \mu^3 .$$

If we take $d = 1.5\,\mu$, $K = 3 \times 10^{-13}$ ergs
$d = 2\,\mu$, $K = 1.3 \times 10^{-13}$ ergs.

2° For frog, we have a dispersion of the values of $\lambda(\omega)$ because, for this large cell, the correlation are studied around different points (r_1) of the surface, where $d(r_1)$ varies from $1.5\,\mu$ to $3\,\mu$ if one excludes the nucleus region. At $\omega/2\pi = 20\,B$ varies from $0.26\,\mu$ to $0.43\,\mu$. This lead to

$$2 \times 10^{-13}\ \text{ergs} < K < 7 \times 10^{-13}\ \text{ergs} .$$

An independent measure of the thickness $d(r_1)$ is necessary to measure K with more accuracy. This case is the most convenient because the frog RBC is large.

3° For chicken, the nucleus region is not negligible compared to the cell dimensions. The nucleus is rigid and the effective thickness $d_e(r_1)$ is smaller than $d(r_1)$. At $\omega/2\pi = 20$ Hz, λ varies from $0.38\,\mu$ to $0.26\,\mu$. This case is more complex, but K is of same order of magnitude ($K \sim 10^{-13}$ ergs).

To conclude, the shape of the correlation function is universal and involve one characteristic length $\lambda(\omega) \sim \omega^{-n}$, with $0.12 < n < 0.19$ in agreement with theoreticial results.

The measure of λ leads to a determination of K in agreement with the expected value. An independent measure of the thickness will be necessary to determinate K with more accuracy.

4.2 THE COMPLETE ANHARMONIC PROBLEM. — Let us return to the full static problem for one interface with arbitrary surface tension σ_0. The free energy is

$$F = \int \left\{ \frac{1}{2}\sigma_0 \,|\, \nabla u \,|^2 + \sigma_1 \,|\, \nabla u \,|^4 + \right. \\ \left. + \frac{1}{2} K \left(\frac{\partial^2 u}{\partial x^2} + \frac{\partial^2 u}{\partial y^2}\right)^2 \right\} \mathrm{d}_2 r . \quad (4.1)$$

Here the σ_1 term includes both rubber distortions and the second order term associated to changes in area.

There is an analogy between this local free energy and the Landau Ginsburg energy for a magnetic phase transition [25] with two components of the magnetisation (M_x, M_y) in a two dimensional space :

$$F = \int \left\{ \frac{1}{2} r_0 (M_x^2 + M_y^2) + u_0 (M_x^2 + M_y^2)^2 + \right. \\ \left. + \frac{1}{2}\left[\left(\frac{\partial M_x}{\partial x}\right)^2 + \left(\frac{\partial M_y}{\partial y}\right)^2\right] \right\} \mathrm{d}_2 r . \quad (4.2)$$

The analog of M_x is $\partial u/\partial x$. The analog of σ_0 is the temperature measured from the mean field transition point $T - T_0$. In both problems there is a quartic coupling, here described by $\sigma_1 (\nabla u)^4$. The analog is not complete, because :

1° in our problem $M_x = \dfrac{\partial u}{\partial x}$ and $M_y = \dfrac{\partial u}{\partial y}$ are not independent but related through $\partial_y M_x = \partial_x M_y$,

2° the gradient term is $\left(\dfrac{\partial M_x}{\partial x} + \dfrac{\partial M_y}{\partial y}\right)^2$ instead of $\left(\dfrac{\partial M_x}{\partial x}\right)^2 + \left(\dfrac{\partial M_y}{\partial y}\right)^2$ in eq. (4.2).

Our harmonic approximation is the analog of the mean field approximation in phase transitions. If we want to go beyond mean field, we have to make use of some general features of correlations as they are known near a critical point. These features can also be expected to hold here :

a) We expect a displacement of the transition point due to the quartic terms : in our problem, this amounts to a renormalisation of the surface tension. The fluctuations change σ_0 into $\tilde{\sigma}_0$ (we give in an appendix a rough calculation of this renormalisation). The crucial point is then the following : the macroscopically observed surface tension is $\tilde{\sigma}_0$ (and not σ_0). In a biconcave cell which can optimise its overall surface, $\tilde{\sigma}_0$ *must vanish* as explained in section 3.1. This means that in our magnetic analog, we must be exactly at the transition point.

b) We would then expect the following behaviour for the correlation function

$$|\, M_x(q) \,|^2 = q^2 \langle\, |\, u_q \,|^2 \,\rangle = \text{const.}\, \frac{1}{q^{2-\eta}} \quad (25)$$

where η is an exponent first introduced by Fisher [25], which measures the deviations from the harmonic approximation. To estimate η we can examine similar magnetic problems in two dimensions; η has been calculated exactly for the Ising Model [25] and $\eta_{\text{Ising}} = \frac{1}{4}$. For the (x, y) *model* [26] ($n = 2$, $d = 2$) yet unsolved, it is believed that $\tilde{\sigma}_0$ is zero not only for one value of T_c, but for a domain of temperature $T < T_c^*$ and η decreases from $\frac{1}{4}$ at $T = T_c^*$ to zero at $T = 0$.

For our problem, η is not known. However, if η is comparable to η_{Ising}, the difference on $\langle | u_q |^2 \rangle$ would not be too serious $\left(\frac{1}{q^4}$ changed into $\frac{1}{q^{4-1/4}}\right)$. This is probably the profond justification of the surprising success of the harmonic approximation.

5. **Conclusion.** — A purely physical interpretation appears sufficient to explain the flicker effect of erythrocytes. The life of the cell is not absolutely fundamental. According to our picture, ghosts should have the same thickness fluctuations. The absence of flicker results from the equality of the refractive indices inside and outside the cell.

The essential physical conditions for Flicker are :

1) Zero surface tension,

2) High fluidity of the cell interior,

3) Inequality of refractive indices.

Conditions 1) and 2) are fulfilled for RBC in physiological conditions. They essentially depend on the overall flexibility of the RBC. This flexibility is necessary for the oxygen transport in capillaries : the flicker effect appears thus as a *secondary feature associated to the central function of the* RBC.

Theoretically, flicker is not specific to RBC. But for most cells the two first physical conditions for flicker are hindered by :

1) a difference in osmotic pressure between the interior and the exterior (membrane under tension),

2) a larger cytoplasm viscosity,

3) the existence of rigid structures at the wall.

Acknowledgments. — The authors are grateful to P. G. de Gennes for many suggestions and comments. One of us thankfully acknowledges the help of Professor M. Bessis and coworkers of the Institut de Pathologie Cellulaire, Hôpital de Kremlin Bicêtre, where the main part of the experimental work has been done.

We are greatly indebted to two referees for very stimulating comments concerning the limitations of the harmonic approximation.

Appendix. — *Mean field estimation of the renormalized surface tension* $\tilde{\sigma}_0$. — To estimate the contribution of the fourth order term, we make a molecular field approximation :

$$| \nabla u |^4 = \langle | \nabla u |^2 \rangle_{\text{th.av.}} | \nabla u |^2 \qquad (1)$$

and F can be written as :

$$F = \int \mathrm{d}_2 r \, \{ (\sigma_0 + \sigma_1 \langle | \nabla u |^2 \rangle | \nabla u |^2 + K(\Delta u)^2 \} . \qquad (2)$$

This expression indicates that the fourth order term leads to a renormalization of the surface tension

$$\tilde{\sigma}_0 = \sigma_0 + \sigma_1 \langle | \nabla u |^2 \rangle . \qquad (3)$$

The assumption that the total surface tension vanishes for the biconcave erythrocyte leads to

$$\sigma_0 + \sigma_1 \langle | \nabla u |^2 \rangle = 0 . \qquad (4)$$

Using this assumption, the elastic energy is again written as (3.1) and we can estimate $\langle | \nabla u |^2 \rangle$ from (3.6) :

$$\langle | \nabla u |^2 \rangle = \sum_q q^2 u_q^2 = \frac{1}{(2\pi)^2} \int 2\pi q \, \mathrm{d}q \, \frac{kT}{Kq^2}$$

$$= \frac{kT}{\pi K} \operatorname{Log} \frac{q_{\max}}{q_{\min}} .$$

Taking $K = 2 \times 10^{-13}$ (which fits our data rather well) and $T = 300\,\text{K}$ ($kT = 5 \times 10^{-14}$ ergs), and $\frac{q_{\max}}{q_{\min}} = \frac{L}{a} = 10^3$, we find $\langle | \nabla u |^2 \rangle_{\text{th.av.}} \simeq \frac{1}{10}$. The negative tension σ_0, which is necessary to cancel the thermal induced surface tension, is thus of the order of several dyne cm^{-1} $\left(\sigma_0 \cong -\sigma_1 \frac{1}{10}\right)$.

Glossary of principal symbols

a	a typical intermolecular distance
a_0	transmission coefficient of the objective
C	surface elastic modulus
d	RBC thickness
e	RBC membrane thickness
F	elastic free energy
$G(r_1\, r_2\, \omega)$	spatial correlation function for the Flicker intensities measured at points r_1 r_2 on the RBC membrane, at a filtering frequency ω.
I	light intensity
k_B	Boltzman constant
K	elastic curvature modulus
L	RBC diameter
n	refractive index
p	pressure

q	wave vector of the mechanical oscillations of the RBC
dS	surface element of the RBC membrane
T	absolute temperature
u	displacement of the RBC membrane
v	velocity of the fluid in the cell
η	viscosity of the interior fluid of the RBC
μ	Evan's shear modulus
λ	light wavelength
λ_ω	correlation length for the thickness fluctuations
σ	surface tension coefficient
$\sigma_{\alpha\beta}$	viscous stress tensor
π_e	external applied pressure
ω	frequency
ρ	density of the cell interior
α_0	retardation angle of the phase plate.

Functional derivative :

$$\frac{\delta F}{\delta u}\left(u, \frac{\partial u}{\partial x}, \frac{\partial^2 u}{\partial x^2}\right) = \frac{\partial F}{\partial u} - \frac{\partial}{\partial x}\frac{\partial F}{\partial\left(\frac{\partial u}{\partial x}\right)} + \frac{\partial^2}{\partial x^2}\frac{\partial F}{\partial\left(\frac{\partial^2 u}{\partial x^2}\right)}.$$

References

[1] BROWICZ, E., *Zbl. Med. Wiss.* **28** (1890) 625.

[2] FORKNER, C. E., ZIA, L. S. and TENG, C. T., *Chin. Med. J.* **50** (1936) 1191.

[3] PULVERTAFT, R. J. V., *J. Clin. Pathol.* **2** (1949) 281.

[4] BLOWERS, R., CLARKSON, E. M. and MAIZELS, M., *J. Physiol.* **113** (1951) 228.

[5] PARPART, A. K. and HOFFMAN, J. F., *J. Cell. Comp. Physiol.* **47** (1956) 295.

[6] PONDER, E., *Haemolysis and related phenomena* (Churchill Ltd, London) (1952).
BESSIS, M., PRENANT, M., *Nouv. rev. fr. Hématol.* **12** (1972) 351 ;
CHAILLERY, B., WEED, R. I., LEBLOND, P. F. et MAIGNE, J., *Nouv. rev. fr. Hématol.* **13** (1973) 71.

[7] For a complete review on RBC and Bibliography, see :
BESSIS, M., *Living blood cells and their ultrastructure* (Springer Verlag, Berlin) 1973.

[8] HELFRICH, W., *Z. Naturforsch*, **28C** (1973) 693.

[9] See : CHAPMAN, D. and WALLACH, D. F. H., *Biological membranes* (edited by D. Chapman, Academic Press, London) 1968.
MC CONNEL, H. and MC FARLAND, B., *Q. rev. Biophys.* **3** (1970) 91.

[10] RAND, R. P. and BURTON, A. C., *Biophys. J.*, **4** (1963) 115 and **4** (1964) 303.

[11] FUNG, Y. C. and TONG, P., *Biophys. J.* **8** (1968) 175.
DANIELSON, D. A., *J. Biomech.* **4** (1971) 611.
BULL, B. *in Red cell shape* (edited by Bessis M and Leblond P., Springer Verlag N. Y.) 1973.

[12] CANHAM, P. B., *J. Theor. Biol.* **26** (1970) 61.

[13] HELFRICH, W. and DEULING, H. J., *Vth international L. C. Conference, Stockholm*, 1974, *J. Physique Colloq.* **C1** (1975) 327.

[14] For a complete review, see DE GENNES, P. G., *The Physics of Liquid Crystals*, Oxford (1974).

[15] DE GENNES, P. G. et PAPOULAR, M., *Vibrations de basse fréquence dans certaines structures biologiques*, Volume jubilaire en l'honneur de A. Kastler (P.U.F. Paris) 1969.

[16] FUNG, Y. C. and ZWEIFACH, B. W., *Annu. Rev. Fluid Mech.* **3** (1971) 189.

[17] LANDAU, L. and LIFCHITZ, E., *Statistical Physics* (Pergamon Press, London) 1959.

[18] KRAMER, L., *J. Chem. Phys.* **55** (1971) 2097.

[19] DE GENNES, P. G., *C. R. Hebd. Séan. Acad. Sci.* **268** (1969) 1207.

[20] BURTON, A. L., ANDERSON, W. L. and ANDREWS, R. V., *Blood*, **32** (1968) 819.

[21] CASPERSON, T., *Exp. Cell. Res.* **7** (1954) 598.

[22] LENNON, J. F., to be published (Thesis) 1976.

[23] BORN, M. and WOLF, E., *Principles of optics* (Pergamon) 1964, p. 427.

[24] HOCHMUTH *et al.*, *J. Biomed.* **5** (1972) 501.
SKALAK *et al.*, *Biophys. J.* **13** (1973) 245.
EVANS, *Biophys. J.* **13** (1973) 926-941.
EVANS and LA CELLE, *Blood* **45** (1975) 29.

[25] STANLEY, H. E., *Introduction to Phase Transitions and Critical Phenomena* (Clarendon Press, Oxford) 1971.
TOULOUSE, G., PFEUTY, P., *Introduction au groupe de renormalisation et à ses applications : phénomènes critiques et autres* (Presse Universitaire de Grenoble) 1975.